High-Pressure Dependence of the Free Volume in Fluoroelastomers from Positron Lifetime and *PVT* Experiments

Günter Dlubek,*,† Jan Wawryszczuk,‡ Jürgen Pionteck,§ Tomasz Goworek,‡ Harald Kaspar,⊥ and K. Helmut Lochhaas⊥

ITA Institute for Innovative Technologies, Köthen, branch office Halle, Wiesenring 4, D-06120 Lieskau (Halle/Saale), Germany, Institute of Physics, Maria Curie-Sklodowska University, Pl. M. Curie-Sklodowskiej 1, PL-20-031 Lublin, Poland, Leibniz Institute of Polymer Research Dresden, Hohe Strasse 6, D-01069 Dresden, Germany, and Dyneon GmbH & Co. KG, Werk Gendorf, D-84504 Burgkirchen, Germany

Received August 17, 2004; Revised Manuscript Received September 14, 2004

ABSTRACT: The microstructure of the free volume and its high-pressure dependence in fluoroelastomeric copolymers of tetrafluoroethylene (TFE) and perfluoro(methyl vinyl ether) (PMVE), PFE, as well as vinylidene fluoride (VDF) and hexafluoropropylene (HFP), VDF/HFP_{22}, was studied by pressure−volume−temperature experiments (*PVT*, $P = 0.1-200$ MPa) and positron annihilation lifetime spectroscopy (PALS, $P = 0.1-448$ MPa, all at 22.5 °C). Employing the Simha−Somcynsky equation of state the excess (hole) free volume fraction h and the specific free and occupied volumes, $V_f = hV$ and $V_{occ} = (1 - h)V$, were estimated from the specific total volume V. The pressure variation of these volumes and their compressibilities are discussed. We found that the occupied volume V_{occ} exhibits a remarkable compressibility, $\kappa_{occ} \approx 2.4 \times 10^{-4}$ MPa^{-1}, while it shows (for $T > T_g$) almost no thermal expansion. The PALS spectra were analyzed using the new routine LT9.0 assuming dispersion in both the positron (τ_2) and orthopositronium (o-Ps) lifetimes (τ_3). We speculate that positrons (e^+) may show Anderson localization at sites of the entire empty volume possibly assisted by an affinity to fluorine atoms. From the o-Ps lifetime parameters the (excess) free volume hole size distribution, its mean value $\langle v_h \rangle$, and dispersion σ_h were calculated. From a comparison of $\langle v_h \rangle$ with V_f the specific hole number N_h' was estimated. N_h' was determined to be constant and the same in compression and thermal expansion experiments. When taking correctly into account the compressibility of the occupied volume V_{occ} the discrepancy in V vs $\langle v_h \rangle$ plots between compression and thermal expansion experiments discussed in the literature disappears.

Introduction

The excess free volume appearing in amorphous polymers due to their structural, static or dynamic, disorder is of fundamental importance for several macroscopic properties of these materials, such as viscosity, structural relaxation, molecular transport and physical aging.[1−5] This excess free volume appears in form of many irregularly shaped, multiconnected local free volumes of atomic and molecular dimension (holes).[6,7] Positron annihilation lifetime spectroscopy (PALS) has developed to be the most important method for studying these subnanometer size holes in polymers.[8,9] PALS itself is able to measure the mean volume of the holes and, with larger limitations, their size distribution,[10,11] but not directly the hole density and the hole fraction. However, by comparing PALS results either directly with the macroscopic volume V[12−16] or with the (excess) free volume V_f, the hole density can be estimated.[15−19]

Cooling and hydrostatic compression of the metastable polymer liquid are two different pathways to form the glassy state. Usually, the free volume is studied as a function of the temperature. High pressure experiments have recently received particular interest for understanding the relaxation dynamics due to the fact that pressure controls molecular packing.[1] However, only a relatively small number of PALS experiments have been performed at high pressure. The work of the Kansas City group is a well-known example, this work revealed a decrease of the mean hole size in polypropylene and epoxy resins with increasing pressure.[8,20,21] The Lublin group studied the effect of pressure on the PALS parameters in various crystalline molecular substances.[22,23] Additionally, some experiments have been performed on pressure-densified polymers.[18]

Recently Bohlen and Kirchheim[14] published macroscopic volume and hole volume (PALS) experiments on polystyrene and polycarbonate. They compared the temperature induced and pressure induced variations of these quantities and estimated that the hole density in compression experiments appears to be more than twice as large as when estimated from the temperature variation. These estimations were interpreted by the authors using a model that assumes the transformation of large to small holes by hydrostatic pressure. The analysis was based on the assumption that the occupied volume does not expand and is not compressible. Recently, some of us have shown that the occupied volume of polymers is distinctly compressible, and taking this into account, it is expected that the discrepancy between compression and thermal expansion experiments disappears.[15,16]

In this paper, we show that this is actually the case. The paper is an extension of a previous work where we have studied the temperature variation of the free volume in two fluoroelastomers using PALS and *PVT* experiments.[24] The fluoroelastomers are ideal systems for this study due to their relatively large holes and

* To whom correspondence should be addressed. Telephone: +49-345-5512902. Fax: +49-40-3603241463. E-mail: gdlubek@aol.com.
† ITA Institute for Innovative Technologies.
‡ Maria Curie-Sklodowska University.
§ Leibniz-Institute of Polymer Research Dresden.
⊥ Dyneon GmbH & Co. KG.

10.1021/ma048310f CCC: $30.25
Published on Web 12/30/2004

Table 1. Sample Characterization and Volume Parameters (at Ambient Pressure and $T = 22.5$ °C) Estimated from the *PVT* Data, where the Compressibilities κ are for $P \rightarrow 0$

denotation	uncertainty	PFE	VDF/HFP_{22}
trade name		Dyneon PFE	Fluorel FC-2175
components		TFE/PMVE	VDF/HFP
molar composition		45−85:55−15[a]	78:22
M_w (kg/mol)	±10%	100	85
T_g (DSC, K)	±1	271	255
V (cm^3/g)	±0.002	0.480	0.554
V_{occ} (cm^3/g)	±0.003	0.431	0.512
V_f (cm^3/g)	±0.003	0.049	0.042
h	±0.003	0.102	0.075
κ (10^{-4} MPa^{-1})	±0.05	8.12	5.38
κ_{occ} (10^{-4} MPa^{-1})	±0.1	2.37	2.10
κ_f (10^{-4} MPa^{-1})	±2	56.9	45.7
T^* (K)	±50	8038	9281
V^* (cm^3/g)	±0.005	0.4493	0.5364
P^* (MPa)	±20	749	850

[a] Exact composition is known to the authors.

completely amorphous nature. In the current work we investigate the free volume in the same fluoroelastomers as a function of hydrostatic pressure.

For the analysis of PALS experiments we used the new routine LT in its latest version 9.0[25,26] which allows both discrete and log−normal distributed annihilation rates. From these distributions the mean size and the size distribution of free volume holes are calculated. *PVT* experiments are analyzed by employing the Simha−Somcynsky equation of state (S−S eos) theory[2−5] (see also our previous papers[15,16,24]). This analysis delivers the fractional (excess or hole) free volume and the specific free and occupied volumes. We show that there is no discrepancy between compression and heating experiments with respect to the mean size, size distribution, and density of free volume holes.

Experimental Section

Samples. The samples under investigation were two commercial fluoroelastomers made by Dyneon GmbH & Co. KG, Burgkirchen, Germany (a 3M Company). One elastomer is a copolymer of tetrafluoroethylene (−[C_2F_4]−, TFE, 45−85 mol %) and perfluoro(methyl vinyl ether) (−[F_2C−CF(OCF_3)]−, PMVE, 15−55 mol %), denoted as Dyneon Perfluoroelastomer PFE (the exact composition is known to the authors). The other elastomer is a copolymer of vinylidene fluoride (−[CF_2CH_2]−, VDF, 78 mol %) and hexafluoropropylene (−[F_2C−CF(CF_3)]−, HFP, 22 mol %), denoted as Fluorel FC-2175 (VDF/HFP_{22}) (see Table 1). In ref 24 more details on the samples and their preparation can be found.

***PVT* Experiments.** The *PVT* experiments were carried out by means of a fully automated GNOMIX high-pressure dilatometer described in our former paper.[24] The instrument is able to detect changes in specific volume as small as 0.0002 cm^{-3}/g with an absolute accuracy of 0.002 cm^{-3}/g.

Positron Lifetime Experiments. The PALS measurements were carried out with a spectrometer which differs from that used in the previous work: a fast−slow coincidence system[9] with BaF_2 scintillators; the time resolution was 230 ps (fwhm of a single Gaussian, ^{22}Na source) and the channel width was 11.8 ps. Two identical samples of 1.5 mm thickness and 20 mm diameter were sandwiched around a 0.5 MBq positron source: $^{22}NaCl$, deposited between two 8 μm thick Kapton sheets. Each sample was covered with an additional 7 μm thick aluminum foil.

The PALS measurements were performed at constant temperature of 22.5(±0.3) °C in the pressure range between 0.1 and 448 MPa (±4 MPa at the highest pressure). For several pressures the measurements were repeated after finishing the first series. The pressure chamber and the experimental arrangement have been described previously.[22,23] Since the detectors had to be placed outside the thick walled pressure chamber, the rate of coincidence counts was significantly reduced and one measurement lasted 12 h.

The spectra which contained ~2×10^6 coincidence counts were analyzed with the routine LT9.0[25,26] assuming three lifetime components. In the final analysis the positron annihilation in the source, 10% of 385 ps (Kapton and NaCl) and 5% of 165 ps (Al foils), was corrected and the resolution function used was determined as a sum of two Gaussians with fwhms of 210 and 280 ps and weights of 80% and 20%, the second Gaussian is shifted by −1.0 channels with respect to the first one (for more details of analysis see ref 24).

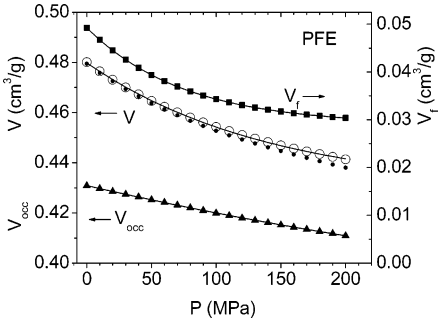

Figure 1. Specific total volume V (open circles) and the specific occupied and free volumes $V_{occ} = (1 - h)V$ (▲) and $V_f = hV$ (■) for PFE at 22.5 °C and increasing pressure. The dots show the volume in the S−S theory fitted to the experimental data below 80 MPa. The lines are first (V_{occ}) or second order (V, V_f) exponential fits.

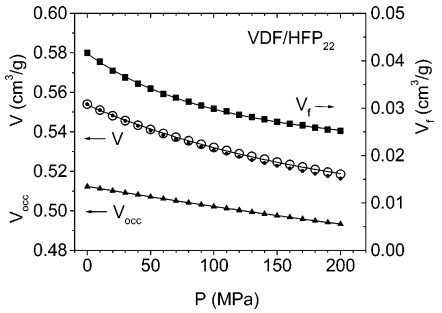

Figure 2. As in Figure 1, but for VDF/HFP_{22}.

Results and Discussion

Specific Total, Free, and Occupied Volume from *PVT* Experiments. Figures 1 and 2 show the pressure dependence of the specific volume V of PFE and VDF/HFP_{22} at a temperature of 22.5 °C. The S−S theory[2] expresses the eos in form of scaled variables, $V/V^* = f(T/T^*, P/P^*)$. We use here the scaling parameters T^* and P^* as determined in ref 24 from fits to the experimental data in the temperature and pressure ranges between 27 and 213 °C and 0.1 and 200 MPa; only V^* is lowered by a small amount of 0.001 cm^3/g (Table 1). With these scaling parameters we calculated the equilibrium volume at 22.5 °C as a function of pressure using the algebraic formula eq 10 in ref 3 (eq 2 in our ref 24). As can be observed in Figures 1 and 2 the calculated volume fits well the experiments in the pressure range between 0.1 MPa and approximately 80 MPa. At higher pressures the fitted curves deviate gradually from the experiments due to the pressure-induced glass transition. The deviation is more clearly visible for PFE due to the higher T_g (Table 1).

As in ref 24 we calculated, using the scaling parameters determined for the liquid, the hole fraction h for both the liquid and the glassy states from a numerical

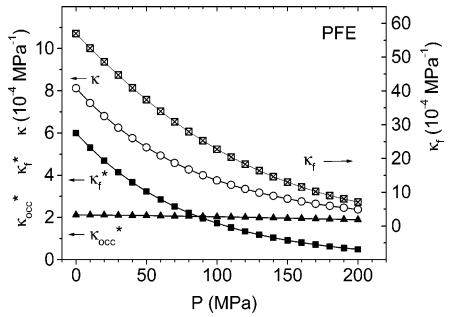

Figure 3. Compressibility of the total, κ (○), and free, κ_f (×-centered open squares), volume and the fractional compressibility of the occupied, κ_{occ}^* (▲), and free, κ_f^* (■), volume for PFE at 22.5 °C.

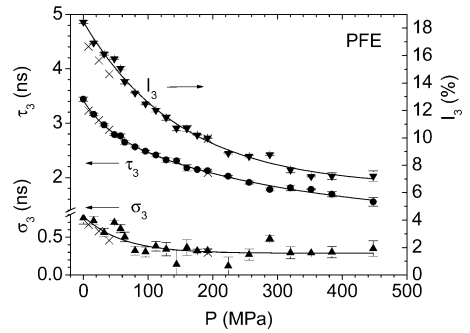

Figure 4. Lifetime parameters of o-Ps annihilation as a function of the pressure P: The mean lifetime τ_3 (●), the dispersion σ_3 (standard deviation of the o-Ps lifetime distribution, ▲), and the relative intensity I_3 (▼) are shown for PFE at 22.5 °C. The lines are first (σ_3, I_3) or second order (τ_3) exponential fits. The crosses show results from a second measurement of the same sample.

solution of eq I in ref 2 (eq 1 in our ref 24). There is no universal relationship for the h-function in the glassy state at present. The S−S eos (eq 1 in ref 24) is derived under the general assumption of equilibrium; however, the specific assumption that the free energy is a minimum has not been made. Therefore, it is usual to calculate the h values from the specific volume below T_g (respectively $T_g(P)$, the pressure dependent glass transition) via this equation assuming constant scaling parameters P^*, V^*, and T^* determined from the specific volume of the liquid. These h values are considered to be sufficiently good approximations for conditions not too far from equilibrium (see detailed discussion by Robertson[4]).

With the knowledge of h the specific excess or hole free volume can be calculated from $V_f = hV$ and the specific occupied volume from $V_{occ} = yV = (1 - h)V$. As in the S−S eos, we assume that the partial volumes V_{occ} and V_f behave additively and are exposed to the same temperature T and hydrostatic pressure P as applied externally to the sample, $V(T, P) = V_{occ}(T, P) + V_f(T, P)$. Under these assumptions, their (fractional) expansivities and compressibilities behave also additively.

The volumes V_{occ} and V_f are shown in Figures 1 and 2 together with the total volume V. As can be observed, V and V_f show an exponential-like decrease with increasing pressure P, while V_{occ} exhibits an almost linear, only weakly curved reduction. For PFE, the specific free volume decreases from 0.049 cm^3/g at ambient pressure to 0.030 cm^3/g at 200 MPa. This corresponds to a decrease in the fractional free volume, $h = V_f/V$, from 0.102 to 0.063. The volumes of VDF/HFP$_{22}$ show a similar variation than of PFE but with higher values for V and V_{occ} and smaller ones for V_f and h. The S−S theory assumes the same cell size for occupied and empty cells. An increase or decrease in V_f comes mainly from the creation or annihilation of empty cells, and to a small portion from the variation of the (uniform) cell size. The variation in the cell volume is mirrored in the variation of the specific occupied volume V_{occ}.

From these data the isothermal compressibility parameters $K = -dV/dP|_T$, $K_{occ} = -dV_{occ}/dP|_T$, and $K_f = -dV_f/dP|_T$ can be estimated. The compressibilities are given by $\kappa = K/V$, $\kappa_{occ} = K_{occ}/V_{occ}$, and $\kappa_f = K_f/V_f$, the corresponding fractional compressibilities by $\kappa_{occ}^* = K_{occ}/V$ and $\kappa_f^* = K_f/V$ with $\kappa_{occ}^* = (1 - h)\kappa_{occ}$, $\kappa_f^* = h\kappa_f$, and $\kappa = \kappa_{occ}^* + \kappa_f^*$ (all at a given T). Figure 3 shows for PFE as an example the behavior of κ, κ_{occ}^*, κ_f^*, and κ_f. Since $V_{occ} \approx V$, $\kappa_{occ} \approx \kappa_{occ}^*$. κ decreases from 8.11 (P = 0.1 MPa) to 2.38 (P = 200 MPa), κ_f from 57.0 to 7.1, all in units of 10^{-4} MPa^{-1}. κ_f^* shows the same behavior as κ, but shifted to lower values by the amount of κ_{occ}^*. The decrease in κ_f^* comes from the decrease in κ_f and in the free volume fraction h.

κ_{occ}^* (κ_{occ}) decreases only slightly, from 2.12 × 10^{-4} to 1.89 ×10^{-4} MPa^{-1} (from 2.37 × 10^{-4} to 2.03 × 10^{-4} MPa^{-1}). These values are similar to those found for polyethylene crystals: 1.5 × 10^{-4} (20 °C) and 1.6 × 10^{-4} MPa^{-1} (66 °C, all for $P \rightarrow 0$).[27] Above a pressure of 80 MPa, κ_f^* is smaller than κ_{occ}^* which is due to the small fractional free volume h. The ratio κ_{occ}^*/κ changes from 0.26 at ambient pressure to 0.85 at 200 MPa. This shows that κ_{occ}^* cannot be neglected in comparison to κ. Therefore, $V_f = V - V_{occ}$ is not the same for the same total volume $V(T, P)$ as frequently assumed but is different for different T, P sets. (Remark: In our previous papers[15,16,24] we have argued that V_f depends on the pathway in the T,P plane. This is a misleading formulation since different pathways can also lead to the same T,P pair.) The compressibilities of VDF/HFP$_{22}$ behave similarly to those of PFE, but are generally smaller.

The Positron Lifetime Spectra and their Analysis. In the lifetime spectrum of amorphous polymers, three exponential-like decay components, $s(t) = \sum(I_i/\tau_i) \exp(-t/\tau_i)$, usually appear. These arise from the annihilation of parapositronium (p-Ps, τ_1), free (not Ps) positrons (e^+, τ_2), and orthopositronium (o-Ps, τ_3; $\tau_1 < \tau_2 < \tau_3$, their relative intensities are $I_1 + I_2 + I_3 = 1$).[9] As we have discussed in detail in our previous paper,[24] physically reasonable lifetime parameters are obtained from the nonlinear least-squares fits to the spectrum when allowing the e^+ and the o-Ps lifetimes to be distributed around their mean values τ_2 and τ_3.

The routine LT9.0 analyzes the dispersion of the lifetimes and returns the standard deviation, σ_2 and σ_3, of their distributions. To improve the statistical accuracy of the analyzed parameters, we reduced the number of free fit parameters by constraining τ_1 to the self-annihilation lifetime of τ_1 = 0.125 ns and the ratio of their intensities, I_1/I_3, to the theoretical ratio of the para/ortho Ps formation probability, $I_1/I_3 = 1/3$ (see the detailed discussion in ref 24). Figures 4 and 5 show the pressure dependence of the o-Ps annihilation for both polymers under investigation. All of these parameters exhibit an exponential-like decrease with increasing pressure.

In amorphous polymers, Ps is formed in subnanometer size holes of the excess free volume or, if formed elsewhere, is trapped by these holes (Anderson localiza-

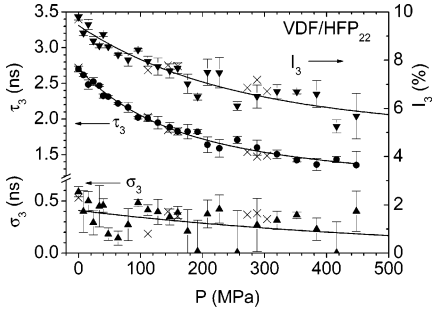

Figure 5. As in Figure 4, but for VDF/HFP_{22}.

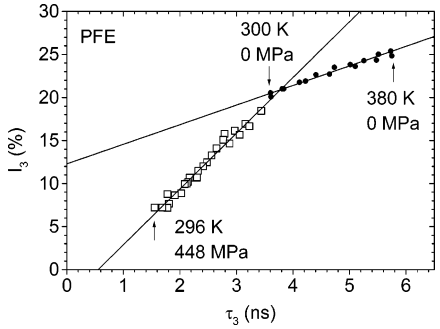

Figure 6. Plot of the intensity I_3 vs the mean lifetime τ_3 of o-Ps annihilation for PFE. Empty squares: current compression experiments at 296 K in the range between 0.1 and 448 MPa: (●) thermal expansion experiments at 0 MPa in the range between 300 and 380 K, from ref 24.

tion[28,29]). This results in the o-Ps lifetime being reduced from its value in a vacuum, 142 ns (self-annihilation), to the low ns range. This is due to the annihilation of o-Ps's positron with an electron other than its bound partner and with opposite spin during a collision with a molecule in the hole wall (pick-off annihilation).[9] The smaller the hole, the higher the frequency of collisions and the shorter the o-Ps life. The dispersion of the o-Ps lifetime has its origin in the size and shape distribution of the free volume holes.[9−11,30] The behavior of τ_3 and σ_3 shows that the mean size of free volume holes and the width of their size distribution decrease with increasing pressure.

We observe in Figures 4 and 5 that the o-Ps intensity, I_3, and lifetime, τ_3, seem to vary in a similar way. The same can be observed in our thermal expansion experiments: I_3 grows with increasing τ_3 and therefore temperature T.[24] Frequently, it is assumed that I_3 shows the variation in the free volume hole density directly.[8] This is misleading, however, as the Ps yield, mirrored by I_3, can be affected by very different processes and properties. Within the radiation chemistry model,[31−33] Ps is formed from a thermal or epithermal positron and an excess electron from the terminal positron spur (blob). This process competes with electron−ion recombination and trapping of e^- and/or e^+ at deep or shallow traps. The up−down−up variation of I_3 with the temperature frequently observed for weakly polar polymers and also poly(tetrafluoroethylene)[34] is explained by trapping-detrapping reactions of spur electrons with shallow traps (radicals) below T_g, and mobilization of ions and their recombination with radicals above T_g.[35] We observed, however, for PFE only a small decrease in I_3 of about 1% over a longer period (compare Figure 4), which we ignore here. VDF/HFP_{22} did not show any observable radiation effect (Figure 5). As usual, we observed no hysteresis in the lifetimes τ_i.

Since our results may indicate that increasing hole size promotes Ps formation we have plotted in Figure 6 I_3 vs τ_3 for PFE as example. A linear dependency is observed with distinctly different slopes for compression and thermal expansion experiments. The question remains how the hole size may effect Ps formation. After the decay of the terminal positron spur a correlated e^+−e^- pair remains if the distance of particles is less than the Onsager sphere. When such a pair occur close to a local free volume they can bind into Ps by passing on to a localized state. The energetic conditions of Ps formation and localization may be describe by[30,31,32]

$$E_+ + E_- > E_{Ps} - I_{Ps} \quad (1)$$

where E are the energies of positrons, electrons, and Ps, measured against the vacuum level, $I_{Ps} \leq 6.8$ eV is the Ps binding energy, and E_{Ps} is the zero-point energy of Ps localized at the hole. In a spherical potential well of finite depth U_0, the minimum well radius at which the energy level exists (i.e. the well is able to trap Ps) is $r_{min} = 2.16$ Å $U_0^{-0.5}$ (U_0 in electronvolts). When assuming $U_0 \approx 3$ eV, the minimum radius of the Ps trap is 1.25 Å. A value of ~1.5 Å has been estimated from experiments.[36] Following Ito[32] the similar variation of I_3 and τ_3 may be the consequence of the hole size distribution: the fraction of holes available for Ps formation (those with a size larger than r_{min}) increases with increasing mean hole size.

Another controlling factor of the process, however, may be the transition rate of particles into the hole. With increasing radius r of the hole the surplus of energy to be dissipated to the bulk, $(E_+ + E_-) - (E_{Ps} - I_{Ps})$, increases since E_{Ps} varies approximately like $1/r^2$.[31] The energy release may occur via the excitation of the large variety of molecular vibrations such as bond stretching, bond-angle bending, and rotational isomeric transitions, as well as localized and cooperative motions of the chains.[37] Electron−hole excitation is usually hindered in insulators due to the large forbidden energy gap between the valence and conduction bands.[38] However, this process may be important in polymers because the structural disorder smears the band structure and creates a lot of deep states lying in the band gap. It has been calculated for small voids in metals, where electron−hole excitation is the dominating process of energy dissipation that the transition rate of positrons increases with the binding energy of positrons at the trap. The result is a linear increase of the trapping (transition) rate with the volume of the void.[39] This result agrees well with experiments (see the review in ref 40 and references given therein). Positron trapping by neutral vacancies in semiconductors was found to show similar properties as in the case of metallic vacancies.[38]

The compression of polymers leads not only to the reduction in the free volume hole size but also to an increasing density of the occupied volume (Figures 1 and 2). This density increase shifts the energy levels of the Ps precursors e^+ and e^- and changes phononic and electronic energy levels as well as the dielectricity constant. During a temperature increase, however, the occupied volume shows almost no change (at ambient pressure and above T_g, see ref 24). This behavior together with a decrease of the radius of Onsager sphere may explain the smaller slope of the I_3 vs τ_3 curve in thermal expansion experiments. We will later show that the number density of free volume holes does not change with pressure or temperature. From this it follows that

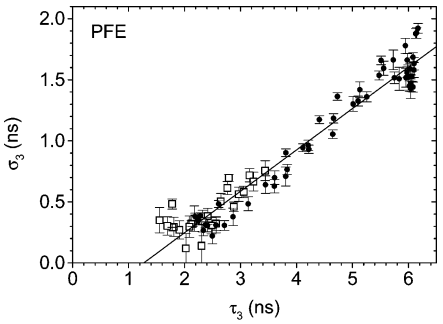

Figure 7. Plot of the dispersion σ_3 vs the mean lifetime τ_3 of the o-Ps annihilation for PFE. Empty squares: current compression experiments: (●) thermal expansion experiments between 100 and 473 K, from ref 24.

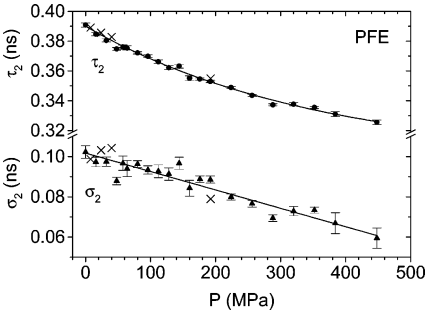

Figure 8. Lifetime parameters of positron (e^+) annihilation as a function of the pressure P: The mean lifetime τ_2 (●) and the dispersion σ_2 (standard deviation of the e^+ lifetime distribution, ▲) are shown for PFE. The lines are first-order exponential fits. The crosses show results from a second measurement of the same sample.

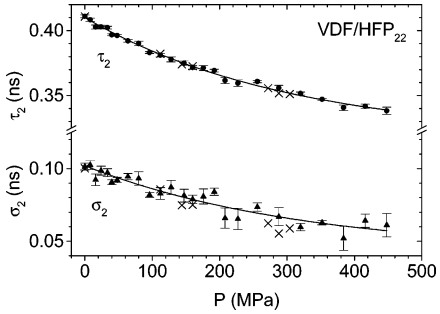

Figure 9. As in Figure 8, but for VDF/HFP_{22}.

I_3 is not simply related to the total number of holes but is strongly controlled by energetic factors including chemical and hole size effects.

It is interesting to compare the variation in σ_3 with that in τ_3. Figure 7 shows for PFE plots of σ_3 vs τ_3 where results from our previous thermal expansion experiments[24] are again included. A good correspondence of both experiments can be observed. σ_3 follows roughly the relation σ_3 (ns) $\approx 0.30(\tau_3 - 0.5)$ (the o-Ps lifetime is 0.5 ns for zero hole volume, see eq 2). A more accurate description is given by σ_3 (ns) $= -0.43(\pm 0.03) + 0.34(\pm 0.01)\tau_3$ where $\tau_3 > 1.26$ ns. The experimental data for VDF/HFP_{22} show a similar behavior, σ_3 (ns) $\approx 0.26(\tau_3 - 0.5)$; the statistical accuracy is, however, smaller due to the small o-Ps intensity I_3 in this polymer.

Figures 8 and 9 show the variation of the positron (e^+) annihilation parameters τ_2 and σ_2 of PFE and VDF/HFP_{22} with the pressure P. Positrons (e^+) annihilate in the empty space between the molecules. The finite width of their lifetime distribution may show that positrons,

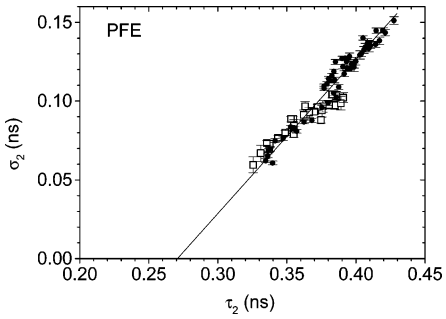

Figure 10. Plot of the dispersion σ_2 vs the lifetime τ_2 of the e^+ annihilation for PFE. Empty squares: current compression experiments: (●) thermal expansion experiments between 100 and 473 K, from ref 24.

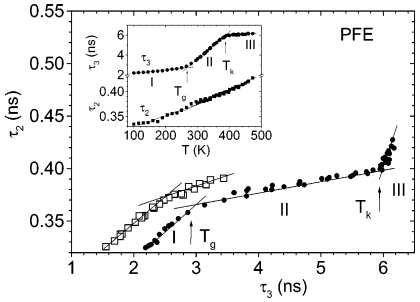

Figure 11. Plot of the mean e^+ lifetime τ_2 vs the mean o-Ps lifetime τ_3 for PFE. Empty squares: current compression experiments, filled circles: thermal expansion experiments. The window shows the variation of τ_2 and τ_3 at zero pressure as a function of temperature, from ref 24.

or at least a fraction of them, are localized in the empty volume at sites of different size. If a positron samples many empty volume sites during its life, the lifetime should be more averaged and not show the dispersion.[29] This conclusion is supported by positron mobility experiments. The mean positron diffusion length has been estimated to be 150 nm in crystalline polyethylene,[41] but ~1 nm in amorphous Kapton.[42]

We observe, however, some differences in the behavior of τ_2 and σ_2 compared with τ_3 and σ_3. The relative variation in τ_2 is smaller than in τ_3 and the pressure dependence of both τ_2 and σ_2 shows a reduced curvature. At room temperature and zero pressure we observe $\sigma_2 \approx 0.25\tau_2$. This ratio, however, changes with the variation of τ_2. From the linear fit shown in Figure 10 one obtains for PFE the relation σ_2 (ns) $= -0.25(\pm 0.01) + 0.93(\pm 0.02)\tau_2$ where $\tau_2 > 0.27$ ns. The data of VDF/HFP_{22} follow σ_2 (ns) $= -0.16(\pm 0.01) + 0.63(\pm 0.03)\tau_2$ where $\tau_2 > 0.25$ ns (not shown).

To understand differences in the positron and o-Ps annihilation in polymers, it is of interest to compare the variations in τ_2 and τ_3. Figure 11 shows a corresponding plot for PFE. The window shows the thermal variation of τ_2 and τ_3 at zero pressure from our previous work.[24] τ_3 exhibits a typical glass transition behavior with a jump-like increase in the coefficient of thermal expansion at T_g (window). At the "knee" temperature T_k the increase of τ_3 levels off. The reason for this behavior, which is not observed in the macroscopic volume, is under discussion.[43] However, it seems clear that above T_k the o-Ps lifetime τ_3 no longer mirrors the correct hole size. The e^+ lifetime shows an almost linear increase with no sign of T_g or T_k.

Because of the different temperature variation of τ_2 and τ_3, the plot of τ_2 vs τ_3 shows three different regions

denoted in Figure 11 as I, II, and III. Between T_g and T_k (region II) τ_2 varies linearly with τ_3 following the function τ_2 (ns) = 0.337(±0.003) + 0.0105(±0.0006)τ_3. When assuming that both e^+ and o-Ps annihilate in the same local free volumes this relation may be used to calibrate τ_2 as a function of the hole volume (see eq 2). It is, however, not clear whether this assumption is correct. In ref 24 we have speculated that positrons (e^+, not Ps) may annihilate in the entire empty space. The continuation in the decrease of τ_2 with decreasing temperature below T_g (region I) without a change in the slope may support this idea.

The entire empty space consists of a large number (volume fraction ≥ 0.26) of small holes forming the *interstitial* free volume and a number of larger holes (volume fraction 0.06−0.1 in our case) forming the *excess* or *hole* free volume (where o-Ps is localized).[15,16] Due to the large fraction of the entire free volume one may expect that positrons rapidly tunnel from hole to hole and form delocalized states. This would actually be the case for periodic potential wells.[29] Then, the positron lifetime would respond to compression or thermal expansion, but not show a distribution. In the case of wells of different size, however, the positron eigenfunctions become predominantly localized in one well or the other so that a positron starting in one well is already in an approximate eigenstate and does not oscillate between wells. This effect is well-known as *Anderson* localization.[28,29] A positron is trapped at only a single hole until it decays. This picture can explain the observed distribution in the e^+ lifetimes.

Above T_k (region III) τ_2 continues its linear increase while τ_3 shows the leveling-off. One explanation of the leveling-off of τ_3 is the assumption that the structural relaxation time comes in the order of the o-Ps lifetime and the holes are smeared during the life of o-Ps.[43] The much shorter living positron (e^+) should be insensitive to this effect and show a continuous increase in τ_2, as observed.

It is not clear at the moment whether the properties of e^+ annihilation observed in this work are of general nature or related to the special type of polymer under investigation. We observed greater similarities between the behavior of τ_2 and τ_3 in poly(dimethylsiloxane) than for the materials in this work. It might be that an affinity of positrons to fluorine atoms, speculated upon in ref 45, assists positron localization at smaller holes.

The τ_2 vs τ_3 plot of the lifetime from pressure experiments (open squares in Figure 11) shows τ_2 values larger than those from thermal expansion experiments by about 0.03 ns. This difference can easily appear due to the use of different lifetime apparatus, source, and background corrections, counting statistics and resolution functions in both experiments. Taking this into account, τ_2 values from pressure and thermal expansion experiments behave in the same way.

Mean Size and Density of Holes. The usual way to calculate the mean radius $r_h(\tau_3)$ of the holes (assumed spherical) at which o-Ps annihilates employs the equation

$$\lambda_{po} = 1/\tau_{po} = 2ns^{-1}\left[1 - \frac{r_h}{r_h + \delta r} + \frac{1}{2\pi}\sin\left(\frac{2\pi r_h}{r_h + \delta r}\right)\right] \quad (2)$$

where $\lambda_{po} = \lambda_3 = 1/\tau_3$ is the mean o-Ps pick-off annihilation rate. This equation comes from a semiempirical model (see refs 8 and 9 and references given therein)

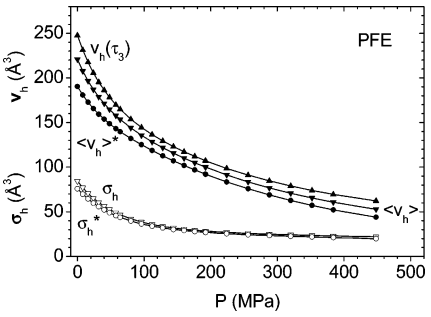

Figure 12. Mean hole volume $\boldsymbol{v}_h$ (filled symbols) for PFE at 22.5 °C, calculated either as $\boldsymbol{v}_h = v_h(\tau_3)$ (▲), the number-average, $\langle v_h \rangle$, of the hole volume distribution $g_n(v_h)$ (▼), or the corrected average volume $\langle v_h \rangle^*$ calculated from the modified distribution $g_n(v_h)^* = g_n(v_h)/v_h$ (●), and the corresponding hole volume dispersions $\sigma_h = \sigma_h$ and σ_h^* (open symbols: ▽, ○) as a function of the pressure P. The lines are second-order exponential fits.

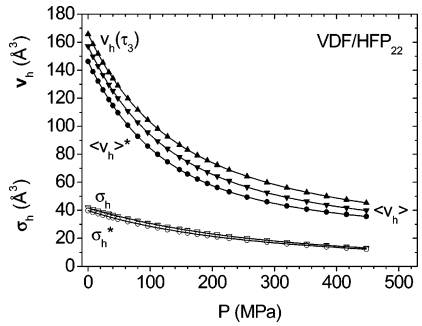

Figure 13. As in Figure 12, but for VDF/HFP$_{22}$.

which assumes that o-Ps is localized in an infinitely high potential well with the radius $r_h + \delta r$ where r_h is the hole radius and the empirically determined δr = 1.66 Å describes the penetration of the Ps wave function into the hole walls. The relation $\lambda_{po} = 1/\tau_{po} = 1/\tau_3$ is based on the assumption that spin conversion and chemical quenching of Ps[9] is negligible. The mean hole volume then follows from $v_h(\tau_3) = (4/3)\pi r_h^3(\tau_3)$.

Since λ_3 and also, therefore, τ_3 have broad distributions, we estimated the mean hole volume as the mass center of the hole size distribution.[24] The radius probability distribution $n(r_h)$ can be calculated from $n(r_h) = -\alpha_3(\lambda)\, d\lambda_3/dr_h$[10,11] where $\alpha_3(\lambda)$ is the o-Ps annihilation rate distribution, which is assumed in the routine LT9.0 to be a log−normal function. The volume fraction hole size distribution follows from $g(v_h) = n(r_h)/4\pi r_h^2$ and the number fraction hole size distribution from $g_n(v_h) = g(v_h)/v_h$. Moreover, as in our previous paper,[24] we calculated the modified distribution $g_n(v_h)^* = g_n(v_h)/v_h$. The mean and the variance of $g_n(v_h)$, $\langle v_h \rangle$, and σ_h^2 and of $g_n(v_h)^*$, $\langle v_h \rangle^*$, and σ_h^{*2} were calculated numerically as first and second moments of these distributions. To reduce the statistical scatter, we have calculated the hole size distributions from τ_3 and σ_3 values smoothed by exponential functions (see Figures 4 and 5). More details about the calculation can be found in ref 24.

Figures 12 and 13 show plots of the mean hole volume for PFE and VDF/HFP$_{22}$, which we denote by the bold symbol $\boldsymbol{v}_h$, calculated either as $\boldsymbol{v}_h = v_h(\tau_3)$, $\langle v_h \rangle$, or $\langle v_h \rangle^*$, and the corresponding hole volume dispersions, $\boldsymbol{\sigma}_h = \sigma_h$ and σ_h^*. Because of the weights $1/v_h$, $\langle v_h \rangle$ is smaller than $v_h(\tau_3)$, and $\langle v_h \rangle^*$ is smaller than $\langle v_h \rangle$. All values exhibit an exponential-like decrease. Below a pressure of 80 MPa there is a transition to the glassy state of the polymer where the hole size displays a continuous

Table 2. Free Volume Parameters (at Ambient Pressure and T = 22.5 °C) Estimated from the PALS Data, where the Hole Compressibilities κ_h are for $P \rightarrow 0$

quantity	uncertainty	PFE	VDF/HFP$_{22}$
$\langle v_h \rangle$ (Å^3)^a	±2	248	166
$\langle v_h \rangle$ (Å^3)^b	±3	221	157
$\langle v_h \rangle$ (Å^3)^c	±5	191	146
κ_h (10^{-3} MPa^{-1})^a	±0.5	8.4	5.7
κ_h (10^{-3} MPa^{-1})^b	±0.6	6.6	n.d.
κ_h (10^{-3} MPa^{-1})^c	±0.8	5.2	n.d.
N_h' (from V_f, 10^{21} g^{-1})^a	±0.01	0.143	0.182
V_{f0} (cm^3/g)^a	±0.002	0.014	0.014
N_h' (from V_f, 10^{21} g^{-1})^b	±0.013	0.169	n.d.
V_{f0} (cm^3/g)^b	±0.003	0.012	n.d.
N_h' (from V_f, 10^{21} g^{-1})^c	±0.015	0.214	n.d.
V_{f0} (cm^3/g)^c	±0.004	0.008	n.d.

^{a} From $v_h(\tau_3)$. ^{b} From $\langle v_h \rangle$. ^{c} From $\langle v_h \rangle$*, see text.

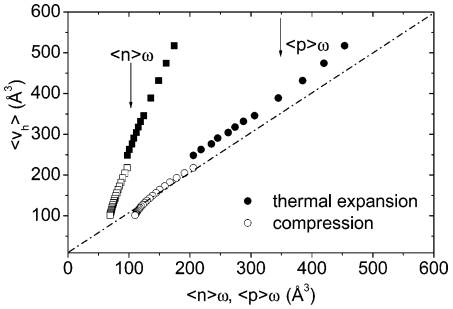

Figure 14. Number-averaged hole volume from PALS, $\langle v_h \rangle$, for PFE vs the volumes $\langle n \rangle\omega$ and $\langle p \rangle\omega$ where $\langle n \rangle$ and $\langle p \rangle$ are the number fraction and volume fraction averaged numbers of S−S vacancies in agglomerates from MC calculations[44] (see also ref 24) and $\omega(P,T)$ is the cell volume. The dash−dot line illustrates a 1:1 correspondence between $\langle v_h \rangle$ and $\langle n \rangle\omega$ or $\langle p \rangle\omega$.

decrease, albeit one with a reduced slope. This behavior is physically reasonable and correlates well with the temperature variation of the hole volume from above to below T_g observed in ref 24. In Table 2, the mean hole volume at 22.5 °C and ambient pressure, v_h, and the hole compressibility $\kappa_h = \boldsymbol{k}_h/v_h$ with $\boldsymbol{k}_h = -\mathrm{d}v_h/\mathrm{d}P$ are shown. One observes that κ_h calculated from $\langle v_h \rangle$* has the same value as κ_f calculated from the *PVT* data (Table 1). The hole volume of VDF/HFP$_{22}$ shows a similar behavior than for PFE but with smaller values of v_h and σ_h.

As discussed in detail in ref 24 the holes detected by o-Ps can be considered as multiples or agglomerates of holes (vacancies) of the S−S lattice (see the Monte Carlo calculations by Vleeshouwers et al.[44]). In Figure 14, we have plotted the number-averaged hole volume $\langle v_h \rangle$ from PALS vs the volumes $\langle n \rangle\omega$ and $\langle p \rangle\omega$ where $\langle n[h(P,T)] \rangle$ and $\langle p[h(P,T)] \rangle$ are the number fraction and volume fraction averaged numbers of S−S vacancies in agglomerates from the MC calculations of Vleeshouwers et al.[44] and $\omega(P,T)$ is the vacancy (cell) volume, $\omega(P,T) = M_0 V_{occ}(P,T)/N_A$ (N_A − Avogadro's number) where $M_0 = RT^*/3P^*V^*$ is the molecular mass of a mer occupying a lattice site (see calculation in ref 24). The cell volume varies at ambient pressure only from ω = 45.2 (300 K) to 45.3 Å^3 (395 K) while it decreases with the pressure from 45.2 (0.1 MPa) to 43.1 Å^3 (200 MPa, all at 22.5 °C). We observe that the plot of $\langle v_h \rangle$ vs $\langle p \rangle\omega$ agrees much better with the expectation of a 1:1 correspondence than $\langle v_h \rangle$ vs $\langle n \rangle\omega$. This behavior supports our conclusion in ref 24 that o-Ps may prefer larger holes with a weight of approximately "v_h". The small deviations from the ideal line and the slight discontinuity between temperature dependent and pressure dependent data can be

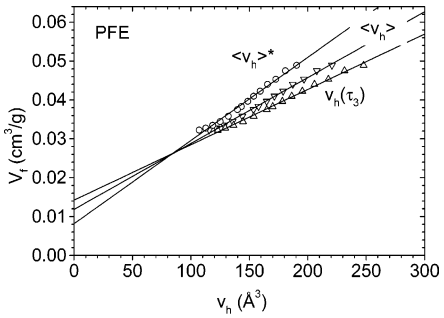

Figure 15. Specific free volume V_f plotted vs the mean hole volume calculated as $\boldsymbol{v}_h = v_h(\tau_3)$ (△), $\langle v_h \rangle$ (▽), or $\langle v_h \rangle$* (○) for PFE (see text). Experimental data from pressure range between 0.1 and 150 MPa.

easily caused by uncertainties in the estimation of τ_3 and σ_3. At higher pressures (smaller $\langle v_h \rangle$) the o-Ps hole volume $\langle v_h \rangle$ seems to decrease faster than $\langle p \rangle\omega$. Further research may clarify this question.

An estimate of the hole density may be obtained by comparing PALS and *PVT* experiments. The mean number of holes per mass unit, N_h', may be determined from one of the relations[12]

$$V_f = V_{f0} + N_h' \boldsymbol{v}_h \tag{3}$$

$$V = V_{occ} + V_{f0} + N_h' \boldsymbol{v}_h \tag{4}$$

where $\boldsymbol{v}_h = v_h(\tau_3)$, $\langle v_h \rangle$, or $\langle v_h \rangle$*. In these equations, the free volume V_f is expressed by $N_h'\boldsymbol{v}_h$. The term V_{f0} may count for a possible deviation of the mean hole volume estimated from the o-Ps lifetime data from the true mean hole volume.

Figure 15 shows, as an example, the specific free volume $V_f = hV$ estimated from the S−S eos analysis of *PVT* data for PFE plotted vs the mean hole volume $\boldsymbol{v}_h$. One observes that V_f follows a linear function of $\boldsymbol{v}_h$, which shows that N_h' does not change with the pressure. The slope of the V_f vs $\boldsymbol{v}_h$ curves, which corresponds directly to N_h', increases when going from $v_h(\tau_3)$ to $\langle v_h \rangle$ and $\langle v_h \rangle$* while the value of V_{f0} decreases (Table 1). As in ref 24, we conclude that $\langle v_h \rangle$* is most compatible with the theoretical expectation that $V_{f0} = 0$. This behavior may again indicate that o-Ps shows a preference for larger holes with a weight approximately equal to the volume of the holes. This preference is corrected in calculating the modified distribution $g_n(v_h)^* = g_n(v_h)/v_h$. The findings $V_{f0} > 0$ may indicate that the correction is not fully complete. Since these conclusions need further evidence we have shown in Figure 15 and in Table 2 all of these three volumes.

There is a complication in the calculation of N_h' for VDF/HFP$_{22}$ which we have already discussed in ref 24. Because of the small values of τ_3 at higher pressures and the finite values of σ_3 the calculated distribution of o-Ps lifetimes extend to values lower than 0.5 ns, the lowest physically reasonable o-Ps lifetime. Because of this effect, the values of $\langle v_h \rangle$ and $\langle v_h \rangle$* are increasingly underestimated with pressure compared with the true values leading to a change in the slope of the V_f vs $\langle v_h \rangle$ and $\langle v_h \rangle$* plots. Therefore, for VDF/HFP$_{22}$, we have only shown results calculated from $v_h(\tau_3)$ (Table 2).

The specific hole number estimated from $\langle v_h \rangle$* for PFE is $N_h' = 0.21(\pm 0.015) \times 10^{21}$ g^{-1}. This value corresponds to a volume related hole density of $N_h = N_h'/V = 0.45(\pm 0.02)$ nm^{-3}. For VDF/HFP$_{22}$ a value of $N_h' = 0.18(\pm 0.01) \times 10^{21}$ g^{-1} (N_h = 0.33 nm^{-3}) is estimated

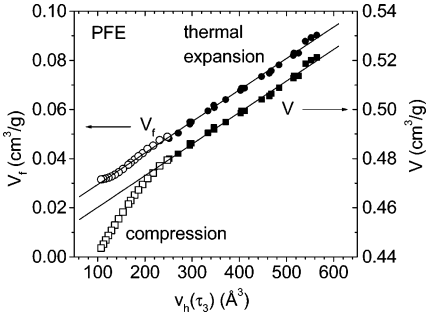

Figure 16. Specific free volume V_f (●, ○) and specific total volume V (■, □) plotted vs the mean hole volume calculated as $v_h(\tau_3)$ for PFE. Open symbols: current compression experiments ($T = 22.5$ °C, pressure range between 0.1 and 192 MPa), filled symbols: thermal expansion experiments ($P = 0.1$ MPa, temperature range between $T_g + 20$ K and T_k) from ref 24. The lines show linear fits to all data (V_f, slope = $0.128(\pm0.01) \times 10^{21}$ g^{-1}) or only to thermal expansion experiments (V, slope = $0.129(\pm0.01) \times 10^{21}$ g^{-1}).

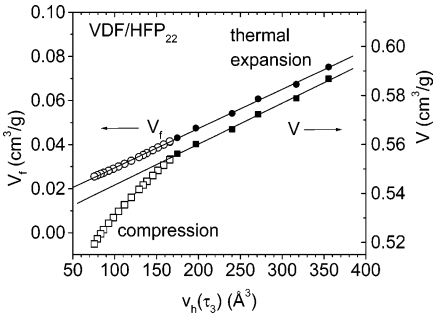

Figure 17. As in Figure 16, but for VDF/HFP$_{22}$**.** The lines show linear fits to all data (V_f, slope = $0.178(\pm0.01) \times 10^{21}$ g^{-1}) or only to thermal expansion experiments (V, slope = $0.173(\pm0.01) \times 10^{21}$ g^{-1}).

from the $v_h(\tau_3)$ data. The hole densities estimated in this paper agree within the error limits with those from our previous thermal expansion experiments.[24]

Plots of the total volume V vs $\boldsymbol{v}_h$ exhibit different behavior from those of V_f: the slopes of the plots increase with increasing pressure (decreasing volume V). Figures 16 and 17 help to understand this behavior and deliver also a direct comparison of isothermal hydrostatic compression and isobaric thermal expansion experiments for both fluoroelastomers. We have plotted the specific free volume V_f and specific total volume V vs the mean hole volume $v_h(\tau_3)$. We look here only to $v_h(\tau_3)$ as example since, as mentioned, slight differences in σ_3 from compression and expansion experiments lead to a discontinuity in the behavior of $\langle v_h \rangle$ and $\langle v_h \rangle^*$. The figures provide evidence that the hole density, N_h', estimated from the slope of the V_f vs $v_h(\tau_3)$ curve is constant and the same in isothermal compression and isobaric thermal expansion experiments.

Assuming constant N_h' its value can be calculated from

$$N_h' = \mathrm{d}V_f/\mathrm{d}v_h = \begin{cases} = \boldsymbol{E}_f/\boldsymbol{e}_h & \text{isobaric thermal expansion} \\ = K_f/\boldsymbol{k}_h & \text{isothermal hydrostatic compression} \end{cases} \quad (5)$$

Here $E_f = \mathrm{d}V_f/\mathrm{d}T$ and $\boldsymbol{e}_h = \mathrm{d}\boldsymbol{v}_h/\mathrm{d}T$ are the thermal expansivities of the specific free, V_f, and hole, $\boldsymbol{v}_h$, volume (P = constant), and $K_f = -\mathrm{d}V_f/\mathrm{d}P$ and $\boldsymbol{k}_h = -\mathrm{d}\boldsymbol{v}_h/\mathrm{d}P$ are the corresponding compressibility parameters (T = constant). While the thermal expansion is almost linear, i.e., E_f and $\boldsymbol{e}_h$ are independent of temperature, the variation of V_f and $\boldsymbol{v}_h$ with the pressure is highly nonlinear (Figures 1, 2, 12, and 13). $K_f/\boldsymbol{k}_h$ is, however, constant as long as $K_f(P)$ and $\boldsymbol{k}_h(P)$ follow the same function. Deviations from the exactly parallel behavior lead to $V_{f0} \neq 0$. Therefore, the values of $K_f(P)/\boldsymbol{k}_h(P)$ have to be averaged over the whole range of data under consideration when calculating N_h' from eq 5.

The (constant) hole density can also be calculated from plots of the specific total volume $V = V_f + V_{occ}$ vs the mean hole volume $\boldsymbol{v}_h$ via

$$N_h' = \mathrm{d}V/\mathrm{d}v_h - \mathrm{d}V_{occ}/\mathrm{d}v_h = \begin{cases} = (\boldsymbol{E} - \boldsymbol{E}_{occ})/\boldsymbol{e}_h & \text{isobaric thermal expansion} \\ = (K - K_{occ})/\boldsymbol{k}_h & \text{isothermal hydrostatic compression} \end{cases} \quad (6)$$

where $E = \mathrm{d}V/\mathrm{d}T$ and $E_{occ} = \mathrm{d}V_{occ}/\mathrm{d}T$ (P = constant) are the isobaric specific expansivities of the total and occupied volume, and $K = -\mathrm{d}V/\mathrm{d}P$ and $K_{occ} = -\mathrm{d}V_{occ}/\mathrm{d}P$ (T = constant) are the corresponding isothermal specific compressibility parameters. In this relation the slope $\mathrm{d}V/\mathrm{d}\boldsymbol{v}_h = K/\boldsymbol{k}_h$ ($\mathrm{d}V/\mathrm{d}\boldsymbol{v}_h = \boldsymbol{E}/\boldsymbol{e}_h$) must be corrected by the term $\mathrm{d}V_{occ}/\mathrm{d}\boldsymbol{v}_h = K_{occ}/\boldsymbol{k}_h$ ($\mathrm{d}V_{occ}/\mathrm{d}\boldsymbol{v}_h = \boldsymbol{E}_{occ}/\boldsymbol{e}_h$) to take into account the possible variation of the occupied volume with the pressure (or the temperature).

The ratio $K/\boldsymbol{k}_h$ grows for PFE with increasing pressure from 0.25×10^{21} g^{-1} at 0.1 MPa to 0.45×10^{21} g^{-1} at 192 MPa. This causes the increasing deviation of the V vs $\boldsymbol{v}_h$ curve from the linear behavior, while the ratio $(K - K_{occ})/\boldsymbol{k}_h = K_f/\boldsymbol{k}_h$ is constant at 0.14×10^{21} g^{-1} (all for $\boldsymbol{k}_h$ calculated from $v_h(\tau_3)$). This behavior leads to an overestimation of the hole density, when being calculated directly from $\mathrm{d}V/\mathrm{d}v_h$, by a factor of 1.5 ($P = 0.1$ MPa, rubbery state) to 2.8 ($P = 192$ MPa, glassy state). These ratios correspond to the values for N_h' estimated in ref 14 from the compression of polystyrene at 390 and 300 K. As we have shown in ref 24, in thermal expansion experiments $\mathrm{d}V_{occ}/\mathbf{d}v_h = \boldsymbol{E}_{occ}/\boldsymbol{e}_h \approx 0.0036 \times 10^{21}$ g^{-1} (for $v_h(\tau_3)$ and $T > T_g$) can be neglected and therefore $\mathrm{d}V/\mathrm{d}\boldsymbol{v}_h = \boldsymbol{E}/\boldsymbol{e}_h$ gives the same good value for N_h' as when estimated from $\mathrm{d}V_f/\mathrm{d}\boldsymbol{v}_h$. This is visualized in the parallel behavior of V and V_f for thermal expansion (Figures 16 and 17). This is not the case below T_g (see refs 15 and 16) and, as we have shown here, generally not for compression experiments.

Conclusion

1. The specific volume V of PFE and VDF/HFP$_{22}$ measured at 22.5 °C as a function of pressure shows an exponential like decrease. This variation can be well fitted by the S−S eos from which the fraction of empty lattice cells, which constitute the excess free volume, is estimated. This fractional excess free volume h was found to vary for PFE between 0.105 at 0.1 MPa to 0.075 at 200 MPa corresponding to a change in specific free volume $V_f = hV$ from 0.051 cm^3/g to 0.0288 cm^3/g. The compressibility of the free volume is 1 order of magnitude larger than that of the total volume V. Both compressibilities decrease exponentially with the pressure. The specific occupied volume V_{occ} shows a definite compressibility with a value similar to that of polymer crystals. The change (at 22.5 °C) is almost linear, from 2.4×10^{-4} to 2.0×10^{-4} MPa^{-1}.

2. The intensity I_3, the mean lifetime τ_3, and the dispersion σ_3 of o-Ps annihilation show an exponential like decrease with increasing pressure. From this a corresponding decrease in the mean hole volume $\boldsymbol{v}_h$ and the standard deviation σ_h of the hole volume distribution follows. From the behavior of τ_2 and σ_2 we speculated that in fluorine polymers positrons (e^+) might undergo Anderson localization at sites of the entire empty space. Possibly an affinity of positrons to fluorine atoms may assist this effect.

3. Plots of the pressure dependent specific free volume $V_f(P)$ vs the hole volume $\boldsymbol{v}_h(P)$ show that the hole density N_h' is constant and the same as found in thermal expansion experiments. Apparent discrepancies between isobaric compression and thermal expansion experiments observed in the literature when plotting the total volume V vs the hole volume $\boldsymbol{v}_h$ have their origin in ignoring the compressibility of the occupied volume V_{occ}.

Acknowledgment. J. Kansy, University of Katowice, is acknowledged for delivering LT9.0 and stimulating discussions to the application of this new routine. We thank D. Kilburn, University of Bristol, for critical reading of the manuscript.

References and Notes

(1) Roland, C. M.; Casalini, B. *Macromolecules* **2003**, *36*, 1361.
(2) Simha, R.; Somcynsky, T. *Macromolecules* **1969**, *2*, 342.
(3) Utracki, L. A.; Simha, R. *Macromol. Theory Simul.* **2001**, *10*, 17.
(4) Roberson, R. E. In *Computational Modeling of Polymers*; Bicerano, J., Ed.; Marcel Dekker: Midland, MI, 1992; p 297.
(5) Utracki, U. A.; Simha, R. *J. Polym. Sci., Part B: Polym. Phys.* **2001**, *39*, 342.
(6) Schmitz, H.; Müller-Plathe, F. *J. Chem. Phys.* **2000**, *112.* 1040.
(7) Hofmann, D.; Entrialgo-Castano, M.; Lebret, A.; Heuchle, M.; Yampolskii, Y. *Macromolecules* **2003**, *36*, 8528.
(8) Jean, Y. C. *Microchem. J.* **1990**, *42*, 72. Jean, Y. C. Positron Annihilation, Proceedings of the 10th International Conference. *Mater. Sci. Forum* **1995**, *175*−*178*, 59.
(9) Jean, Y. C.; Mallon, P. E.; Schrader, D. M., Eds.; *Principles and Application of Positron and Positronium Chemistry*; World Scientific: Singapore, 2003.
(10) Gregory, R. B. *J. Appl. Phys.* **1991**, *70*, 4665.
(11) Liu, J.; Deng, Q.; Jean, Y. C. *Macromolecules* **1993**, *26*, 7149.
(12) Dlubek, G.; Stejny, J.; Alam, M. A. *Macromolecules* **1998**, *31*, 4574.
(13) Srithawatpong, R.; Peng, Z. L.; Olson, B. G.; Jamieson, A: M.; Simha, R.; McGervey, J. D.; Maier, T. R.; Halasa, A. F.; Ishida, H. *J. Polym. Sci., Part B: Polym. Phys.* **1999**, *37*, 2754.
(14) Bohlen, J.; Kirchheim, R. *Macromolecules* **2001**, *34*, 4210.
(15) Dlubek, G.; Pionteck, J.; Kilburn, D. *Macromol. Chem. Phys.* **2004**, *205*, 500.
(16) Dlubek, G.; Bondarenko, V.; Al-Qaradawi, I. Y.; Kilburn, D.; Krause-Rehberg, R. *Macromol. Chem. Phys.* **2004**, *205*, 512.
(17) Yu, Z.; Yashi, U.; McGervey, J. D.; Jamieson, A. M.; Simha, R. *J. Polym. Sci., Part B: Polym. Phys.* **1994**, *32*, 2637.
(18) Schmidt, M.; Maurer, F. H. J. *Macromolecules* **2000**, *33*, 3879.
(19) Schmidt, M.; Maurer, F. H. J. *Polymer* **2000**, *41*, 8419.
(20) Deng, Q.; Sundar, C. S.; Jean, Y. C. *J. Phys. Chem.* **1992**, *96*, 492.
(21) Deng, Q.; Jean, Y. C. *Macromolecules* **1993**, *26*, 30.
(22) Goworek, T.; Zaleski, R.; Wawryszczuk, J. *Chem. Phys.* **2003**, *295*, 243.
(23) Goworek, T.; Wawryszczuk, J.; Zaleski, R. *Chem. Phys. Lett.* **2004**, *387*, 433.
(24) Dlubek, G.; Sen Gupta, A.; Pionteck, J.; Krause-Rehberg, R.; Kaspar, H.; Lochhaas, K. *Macromolecules* **2004**, *37*, 6606.
(25) Kansy, J. *Nucl. Instrum. Methods A* **1996**, *374,* 235.
(26) Kansy, J. *LT for Windows, Version 9.0*. Instute of Physical Chemistry of Metals, Silesian University, Bankowa 12, PL-40-007 Katowice, Poland, March 2002, private communication.
(27) Jain, R. K.; Simha, R. *J. Polym. Sci.: Polym. Lett. Ed.* **1979**, *17*, 33.
(28) Anderson, P. W. *Phys. Rev.* **1958**, *109*, 1492.
(29) Baugher, A. H.; Kossler, W. J.; Petzinger, K. G. *Macromolecules* **1996**, *29*, 7280.
(30) Goworek, T. *J. Nucl. Radiochem. Sci.* **2000**, *1*, 11.
(31) Mogensen, O. E. *Positron Annihilation in Chemistry*; Springer-Verlag: Berlin, Heidelberg, Germany, and New York, 1995.
(32) Ito, Y. *Mater. Sci. Forum* **1995**, *175*−*178*, 627.
(33) Stepanov, S. V.; Byakov, V. M. *J. Chem. Phys.* **2002**, *116*, 6178.
(34) Dlubek, G.; Saarinen, K.; Fretwell, H. M. *J. Polym. Sci., Part B: Polym. Phys.* **1998**, *36,* 1513.
(35) Hirade, T.; Maurer, F. H. J.; Eldrup, M. *Radiat. Phys. Chem.* **2000**, *58*, 465.
(36) Jasinska, B.; Koziol, A. E.; Goworek, T. *Acta Phys. Pol., A* **1999**, *95*, 557.
(37) Tanabe, Y. In *Macromolecular Science and Engineering*; Tanabe, Y., Ed.; Springer-Verlag: Berlin, Heidelberg, Germany, and New York, 1999; p 267.
(38) Puska, M. J.; Nieminen, R. M. *Rev. Mod. Phys.* **1994**, *66*, 841.
(39) Nieminen, R. M.; Laakkonen, J. *Appl. Phys.* **1979**, *20*, 181.
(40) Hautojärvi, P.; Corbel, C. In *Positron Spectroscopy of Solids, Proceedings of the International School of Physics "Enrico Fermi"*; Course CXXV, Varenna, Italy, July 6−16, 1993; Dupasquier, A.; Mills, A. P., Jr., Eds.; IOOS Press: Amsterdam, 1995; p 491.
(41) Brusa, R. S.; Duarte Naia, M.; Margoni, D.; Zecca, A. *Appl. Phys. A: Mater. Sci. Process.* **1995**, *60*, 447.
(42) Brusa, R. S.; Dupasquier, A.; Galvanetto, E.; Zecca, A. *Appl. Phys. A: Mater. Sci. Process.* **1992**, *54*, 233.
(43) Dlubek. G.; Supej, M.; Bondarenko, V.; Pionteck, J.; Pompe, G.; Krause-Rehberg, R.; Emri, I. *J. Polym. Sci., Part B: Polym. Phys.* **2003**, *41*, 3077.
(44) Vleeshouwers, S.; Kluin, J.-E.; McGervey, J. D.; Jamieson, A. M.; Simha, R. *J. Polym. Sci., Part B: Polym. Phys.* **1992**, *30*, 1429.
(45) Dlubek, G.; Fretwell, H. M.; Alam, M. A. *Macromolecules* **2000**, *33*, 187.

MA048310F